

Computer-aided diagnostic system kinds and pulmonary nodule detection efficacy

Omar Raad Kadhim, Hassan Jassim Motlak, Kasim Karam Abdalla

Department of Electrical Engineering, College of Engineering, University of Babylon, Babylon, Iraq

Article Info

Article history:

Received Mar 28, 2021

Revised Jun 17, 2022

Accepted Jun 27, 2022

Keywords:

Computed tomography

auto-encoders

Computer-aided detection systems

Convolution neural network

Stacked auto-encoders

ABSTRACT

This paper summarizes the literature on computer-aided detection (CAD) systems used to identify and diagnose lung nodules in images obtained with computed tomography (CT) scanners. The importance of developing such systems lies in the fact that the process of manually detecting lung nodules is painstaking and sequential work for radiologists, as it takes a long time. Moreover, the pulmonary nodules have multiple appearances and shapes, and the large number of slices generated by the scanner creates great difficulty in accurately locating the lung nodules. The handcraft nodules detection process can be caused by missing some nodules spicily when these nodules' diameter be less than 10 mm. So, the CAD system is an essential assistant to the radiologist in this case of nodule detection, and it contributed to reducing time consumption in nodules detection; moreover, it applied more accuracy in this field. The objective of this paper is to follow up on current and previous work on lung cancer detection and lung nodule diagnosis. This literature dealt with a group of specialized systems in this field quickly and showed the methods used in them. It dealt with an emphasis on a system based on deep learning involving neural convolution networks.

This is an open access article under the [CC BY-SA](https://creativecommons.org/licenses/by-sa/4.0/) license.



Corresponding Author:

Omar Raad Kadhim

Electrical Engineering, Babylon University

Babylon, Iraq

Email: omaryo.omar@gmail.com

1. INTRODUCTION

Cancer can be considered the second-largest mortality cause worldwide. The number of deaths caused by this disease is estimated to be 1 per 6 mortalities at the international level. Moreover, approximately 9,6 million fatalities in 2018, as shown in the World Health Organization (WHO) reports [1]. Lung cancer is amongst the most prevalent types of cancer in the world, with a high rate of infection for both sexes alike. We can verify this through the data provided by the International Agency for Research on Cancer (IARC) for the year 2018 [2]. The data of this agency showed that lung cancer takes the lead the remainder of the injury types of cancer; furthermore, it showed that the incidence of lung cancer reached (11.6 percent) from totally registered cancer cases. The agency reports indicated that the number of injuries reached more than (2,093,876), distributed by (1,368,524) injuries in men and (725,352) injuries in women. On the other hand, according to (IARC), the total number of deaths worldwide in 2018 (1,761,007) as a result of lung cancer. Tobacco consumption is one of the most severe factors that cause cancer, and tobacco is responsible for an estimated 22% of cancer deaths.

The mortality of cancer can indeed be decreased by the early diagnosis and treatment of cases. So, for earlier detection, several ways to screen lung cancer are utilized, for example, a biopsy, computed tomography scans, radiography, and sputum cytology, which doctors recommend among the various

ways [2]. The usual method is computed tomography scanning, and the updated screening technology is the low-dose computed tomography (LDCT) [3]. The adoption of LDCT protocols to screen lung cancer is an effective way to detect lung nodules early. However, there are many obstacles in this type of diagnosis, including [1] the negative impact on low disparity lesion visibility due to low dose spatial imaging resolution and noise is growing. This presents defiance for radiologists to find small nodules and try to interpret them [2]. Moreover, it is also a challenge for radiologists to decide whether a node is malignant or benign in interpreting LDCT scans [3]. Furthermore, results may be susceptible to error due to manual reading or due to many cases number, and the radiologists can lose nodules and thus possible cancer. The exposure to radiation in a low-dose computed tomography scan ranges from 1 to 4 millisieverts [3]. If the scanning process has a positive result, it is especially recommended to low-dose CT screening [4]. The risk that older patients will develop cancer can be increased due to repeated computed tomography scans. To reduce frequent computed tomography scanning, several researchers developed systems known as computer-aided detection (CAD), which can contribute to reducing false-positive discovery and increased sensitivity in cancer diagnosis. As lung cancer deaths have increased, extensive research has been undertaken since 2009. Based on the information presented above, the mortality rate can be decreased or treat this type of cancer if it is detected early and precisely. This is what CAD systems attempt to provide.

In this paper, the crux of the research problems revolves around: firstly, the diversity of CAD systems and the various approaches utilized in them, and how utilized a proper technique. Secondly utilizing the (CAD) systems developed by researchers, there was a variation in diagnostic results for cancerous nodules in the lung in terms of sensitivity and accuracy of these systems. The objective of this paper is to investigate several kinds of CAD systems and try to focus on some details to assess the efficiency of the mechanisms. Finally, the performance of some CAD systems proposed in the literature are compared methods is compared in terms of specificity, accuracy, and sensitivity.

2. METHODS

This section of the paper overview and describes previous literary works, techniques, and methods used by researchers at the various stages of CAD systems. It deals with each stage according to what was stated in the previous literature; furthermore, it gives a brief introduction about each stage. But before starting to describe the CAD systems, it is necessary to describe the data packets entering these systems and processed by the CT scanner.

2.1. Data acquisition

The availability of several public websites hosting huge medical image repositories related to all lung diseases is a promising attempt to enhance lung cancer research. It is therefore noted that most researchers in the field of computer-aided detection (CAD) systems have developed their systems based on the databases and medical images available at these sites. So, firstly, the medical CT images are collected from these public repositories and adopted to the computer-aided detection (CAD) system. These images are in a digital imaging and communications in medicine file format (DICOM). When the work concerns lung nodules detection, the CT images are usually (512 by 512) pixels in the shape of a two-dimensional slice. Slices vary in number between one scan and another. It is also worth noting are some of these essential sites which provide medical images, to name a few (LIDC-IDRI) repositories [1] and The automatic nodule detection 2009 (ANODE09) databases [2].

2.2. CAD system

A brief introduction is discussed in this section about the formation of (CAD) system. CAD systems are classified into two forms, as shown in Figure 1, depending on the feature extraction method that is utilized to extract the lung nodules. The first one is well known as a Handcraft or traditional-CAD system, which utilizes manual feature extraction, and the second one is adopted deep learning spatially convolution neural network (CNN) to learn these features automatically. In this paper, these two systems will be reviewed, and a comparison made based on what researchers presented in these two fields.

2.2.1. CAD system utilized handcraft or traditional feature extraction

These systems utilized handcrafted features extracted to specify malignant tissue and benign tissue. The images obtained from a CT scan in these systems are often handled in four main stages. The first one is noise denoising and images enhancements (pre-processing). After that, the second stage is a segmentation of the lungs, the third stage deals with detecting nodules. Finally, the fourth stage deals with the nodule classification if it is benign or malignant Figure 2. Each stage was precisely described by looking at the related works so far.

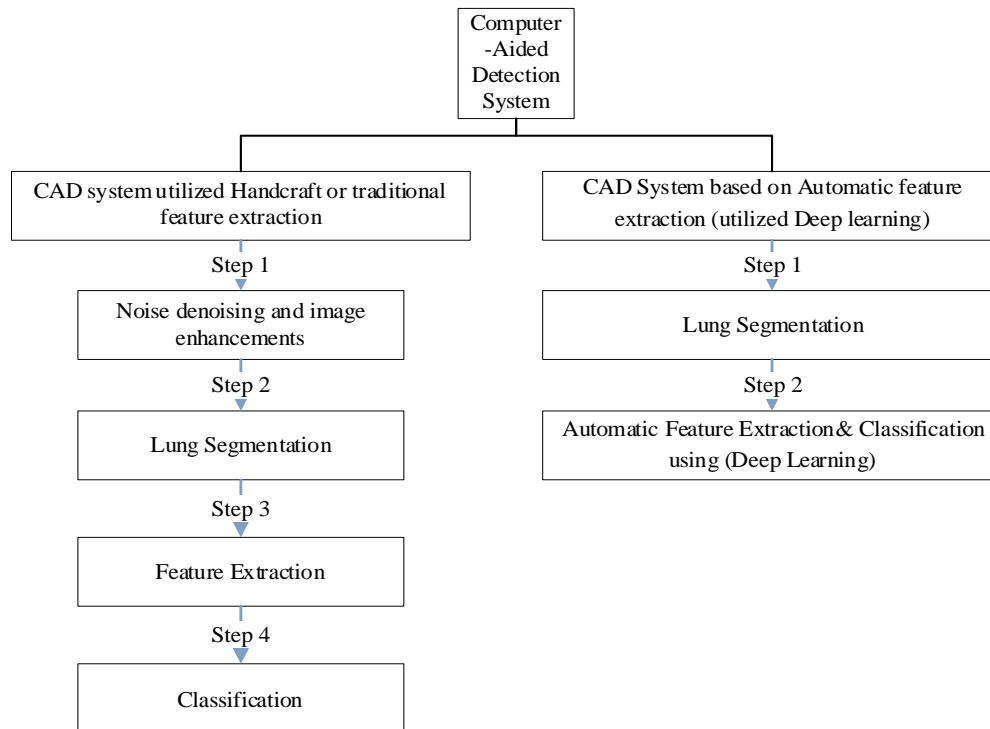


Figure 1. CAD systems classification

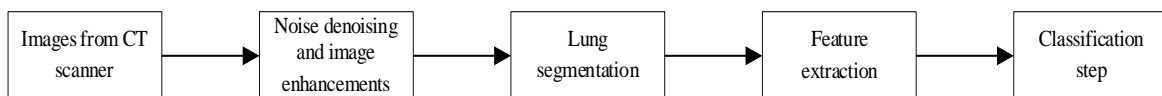


Figure 2. CAD system based on handcraft or traditional feature extraction

a. Noise denoising and image enhancements

This stage is a pre-processing stage and can be done by implementing a variety of types of filters, which can contribute to reducing the noise and enhancement computed tomography scan images. The literature contains various filters, among them the log filter, Gaussian and median filter, and dot enhancement filter, and in the pre-processing stage, histogram-based filters are frequently adopted. Log filter is adopted in [5]–[7]. Gaussian filter is adopted in the work of [8], [9]. The median filter has been adopted in [9]–[13]. In other literature, the dot enhancement filter was adopted in [14], [15]. Wiener filter was examined in [11]. The multi-scale filter was examined in [16], [17]. Wiener filter with contrast limited adaptive histogram equalization (CLAHE) is applied in [14]. The selective enhancement filter is applied in [18]–[20]. A multi-scale selective enhancement filter was applied in [14]. Gabor filter was examined in [17]. Local binary patterns (LBP) filter was used in [18], fuzzy filter adopted in [19], the sequential filter was implemented in [20] was used as a pre-processing step Shell filter examined in [21].

b. Lung segmentation

This stage's goals are to increase the ability of lung nodules detections, and this is done by reducing the search area. So, several steps are followed to get lung segmentation properly. To achieve the lung segmentation stage sub-steps are utilized to images. The first sub-step is extracting thorax from a computed tomography scan: In this phase, cleans and removes all things outside the patient's body. For instance, the place where the patient lies, the bedsheets, and the air in its [22]. The second sub-step is to extract the left and right lungs only, and this can be achieved by adopting the Hounsfield method to CT scan images. These images' histograms after hounsfield are divided into a variety of voxel intensities. The lungs with low voxel intensity are with a range from -900 to -500 HU. The other higher voxel intensity with a value above the -500 HU, for instance, blood, fat, bone, muscles, and chest wall. The threshold is made to isolate lung parenchyma. The -500 HU value is used as an ideal thresholding value by many researchers or optimal

threshold computed by adopting iterative optimal threshold methods. After that, a region growing algorithm is adopted to reconstruct the lungs depending on the most significant region, representing the first lung, and the second biggest one represents the second lungs. Thus, by designing a proper mask, the two-lung region (left & right) can be extracted from a computed tomography slice. For lung segmentation, a region-growing algorithm, in addition to a threshold as stopping criteria, can be implemented, as described in [22]. Several studies have used a 3D region-growing algorithm for pulmonary segmentation. The image labels after segmentation by using a 3D labeling algorithm. In the end, two lung regions were extracted from the labeled image, the largest and next largest connected regions, and the rest of the segmented regions set as the background [23], [24]. The threshold segmentation of the lungs is the work of [18], [19], [21]–[23], [25]–[27], [28]–[36]. Otsu threshold [28], [37], segmentation on the basis of the iterative threshold [9], [38], [39], adaptive threshold [26], [40], The literature has an adaptive 3-D fuzzy threshold [41]. Pulmonary segmentation on the basis of region and 3D region can be located in [5], [42]–[48]. A global active contour method for lung segmentation is discussed in [24].

c. Feature extraction

The significant benefit of this phase is to eliminate or reduce false-positive lung nodule detection. Several features' kinds are presented in the literature. Furthermore, these features are classified as nodules depending on shapes, texture, and intensity. The first feature depending on the shape, especially the morphology of the nodule, is a circular in 2D CT scan or spherical morphology in 3D CT scan, and the second feature depends on the texture. Another extracted feature is the intensity feature. The extracted vector of this feature is then fed to the final step (classification step) to decide the nodule if it is benign or malignant. Some of the literature showed that the reduction of false-positive nodules detection could be made through extracting more than feature types, for instance, the shape and the texture features. In [25], texture features like (Shannon and Tsallis Q entropy) are adopted. In [49], Shannon entropy, Gaussian smoothing, Kullback and Leibler divergence method, Canny edge detection, Gaussian filter, and double thresholding method are adopted to extract features from CT scan images. In [50], several features are adopted, for instance, grey value features, shape features, the position of each region of interest (ROI), computed tomography min value, computed tomography max value, volume sphericity, spatial distribution density, and maximum diameter feature. In [51], area feature is utilized, pixel mean intensity, and centroid, finally, diameter and perimeter eccentricity feature used in this work. In [52], the shape feature, besides several features such as grey-level and surface feature, gradient feature, texture feature, and forward-backward feature selection, is utilized in this work. In [53], the alpha shape method is adopted. Besides shape feature, texture feature and a combination between shape and texture feature vectors are utilized to feed the classifier later. In [9], surface saliency and surface-normal vector, and applied novel feature, wall detection, and elimination and angular histogram of surface normal (AHSN) to extract features from CT scan images. Finally, the comparison is held between the novel feature and others. In [54] diversity index feature, ring feature, and sphere feature are used in this work. In [55], the Gaussian mixture feature and rule-based filtering are implemented in this work. In [56] Shape diagram, 3D proportion measurement is used, and the 3D cylindrical approach is utilized in this work. Appearance feature, morphology feature, texture feature, grey-level feature, two-dimensional feature, long axis feature, short axis feature, perimeter feature, area feature, three-dimensional shape, barycenter difference feature are implemented in the work of [13].

d. Classification step

At this phase, the features vectors obtained in the previous step are classified through two sub-stages. The first phase investigated whether or not the ROI is a nodule, so this can be assumed reducing in the false positive, and this can increase the specificity for a CAD system. The second stage examines if the nodule is classified as benign or malignant. The k-means clustering is implemented to segmentation of juxtavascular and juxtapleura nodules, and it takes less time when compared with other methods [30]. In [50], rule-based classification (RBC) is utilized to minimize the false-positive rate and classify nodules correctly. Furthermore, a comparison is made with k-nearest neighbors and neural networks. Several researchers are adopted the space vector machine (SVM) classifier to reduce the false-positive rate and examine if nodules are malignant or benign. In [52], a novel method is adopted to decrease the false-positive ratio, so the classifier implemented to classify nodule is SVM with Massive training artificial neural network (MTNN). In [53], the generalized linear model regression (GLMR) classifier is implemented and compared with the other classes. After this step, the detection of nodules from non-nodule is done, and the performance for the system must be calculated.

2.2.2. CAD system based on automatic feature extraction (utilized deep learning)

Due to the differences observed in the complexity of biomedical images, medical things, for example, lesions and anatomy are difficult to recognize from the picture. Therefore, instead of seeking

excellent features based on manual extracting, there has been an emphasis on the automatic method of functional learning known as (learning example). Furthermore, deep learning algorithms have become a precious tool for medical imagery utilized for detection, characterization, and analysis the lesions. This method involved developing layer-specific network architecture by taking into account the aim of increased prediction performance. In this type of system, two models can be achieved. First, no manual vector of feature extraction is used because a deep learning algorithm depends on a U-net network to extract nodules masks in lung segmentation steps and then feed them directly to another neural network to classify them. The second model deals with feeding the images after pre-processing techniques directly to the neural network and taking the image as pixels to detect nodules. Figure 3 views the architecture for this technique. However, there are two kinds of deep learning classified depending on the training method. The first one is a supervised method that needs a training data set to learn from it, for example, of these networks (MTNN), convolution neural networks (CNN). In contrast to supervised networks, the unsupervised deep learning method never need to data set for learning from it and directly fed the images to the network, for instance, of these networks (AEs) auto-encoders and (SAEs) stacked auto-encoders. A survey was conducted on deep learning in various network architectures with medical imaging implementations is utilized in [57]. The latest enhancement and challenges in medical imagery machine learning are discussed in [58], [59]. Previous literature has shown that method convolution neural network is a promising method with valuable medical results. It has, therefore, been included in many works of literature. Various kinds of it can be constructed According to the number of classes and layer dimensions. In previous literature, this method was applied to the form (2-D CNN), and the second form is (3-D CNN).

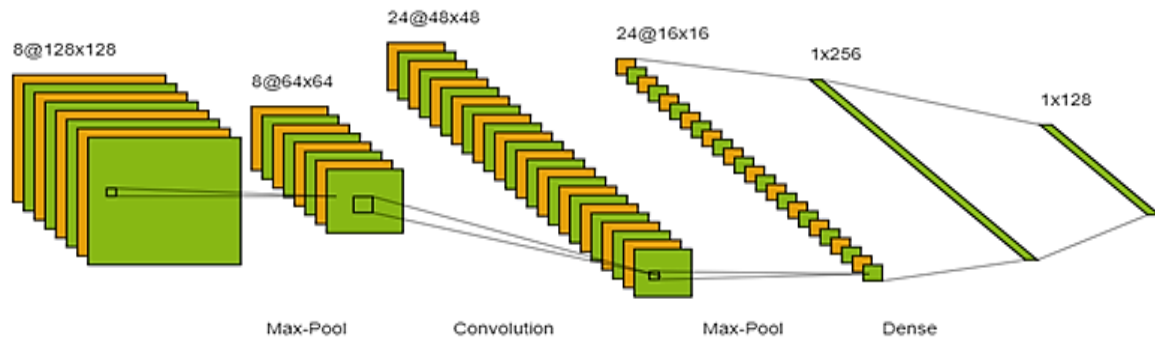


Figure 3. Deep learning network

a. CNN based on a 2-dimension image

In this method, the essential 2-D conversion procedure was being utilized to detect local characteristics of the whole image. For its computational efficiency and simplicity, CNN architecture uses this mostly. Images in tradition contain an intensity matrix, and these images are 2-D dimensions. In this network, it automatically learned to various 2-D features/filters from the training dataset. Several 2-D convolution Nets streams are proposed in [60]. In the beginning, three algorithms for candidate detectors specially designed for finding sub-solid, massive, and solid nodules were combined. Then, a 2-D patches group with 64x64 pixels was taken away from distinct, focused planes for each candidate. In [61], the data are from two sources PET/CT scans images after filtered fed to CNN to detect nodules and finally used SVM classifier. In [62], U-net architecture is adopted for image segmentation. This method is used to extract the high-level information by contracting path and the other path, which is the symmetric expanding path used to reconstruct the information needed. In [63], several models of convolution neural networks are implemented, such as LeNet, VGG-16 deep learning, and AlexNet in the final, the fully connected layer output is applied directly to various classifiers, and comparisons are held between these classifier outputs to select the best methods. In [64], 2-D CNN is adopted with two ROI sizes; the first one is 32*32, and the second is 64*64. Furthermore, the architecture for this neural network depends on two convolution layers. The first convolution layer is adopted with eight feature maps at the same time; the second contains sixteen feature maps. The convolution layers are followed by the downsampling layer with kernel size 2*2. Finally, four layers are fully connected, attached to the final downsample layer. The first one fully connected layer contains 150 nodes, while the second layer has 100 nodes, also the third layer deals with 50 nodes; finally, the last layer deals with two nodes to make a final decision. In [65], a cascade of neural networks with selective classifiers are adopted. This implementation is used to address the class imbalance problem.

b. CNN based on a 3-dimension image

The fundamental convolution operation was considered in three directions (x, y, z) simultaneously in this network. The 3-D convolutional filters implement and have been used for automatic extraction via the input 3-D data. These networks cost more than 2-D networks in terms of calculation efficiency. 3-D convolution operations require further memory, while a 3-D matrix calculation is necessary to save features extracted in the memory of the computer. The main 3-D CNN benefit is that with 3-D filters, it provides multi-view features. Lung nodule detection architecture based on 3-D CNN, proposed by [66]. There are Three 3-D CNNs used by researchers to representative features and encode spatial information by adopting a hierarchical structure, in the first structure, using a field size of $20 \times 20 \times 6$, the second structure with size $30 \times 30 \times 10$, finally third structure with field size $40 \times 40 \times 20$. After that, these structures are merged and made a feature extractor system. In [67], 3-D CNN is adopted with multi-level contextual. Due to variation in the size of nodules, so four various size of 3-D CNN is designed and the fusion for these networks give an excellent coverage error for classifiers.

2.3. Summarized CAD systems

The performance of a CAD system employing Handcraft or conventional feature extraction is dependent in some way on the processing steps performed before the feature extraction step. Therefore, CT scan images are passed through the image enhancement and image segmentation processes. In order to prepare the region of interest (ROI) for feature extraction, approaches chosen during the enhancement and segmentation steps are sometimes manually and precisely tuned. While the CAD system based on automatic feature extraction (using deep learning) (the second module) employs an automatic features extractor, each image pixel is analyzed, and the best features are extracted directly. The automatically features extracted can reduce the requirement for image enhancement and segmentation techniques. Therefore, the time consumption is decreased. Table 1 classified these techniques based on feature extraction methods which is utilized in previous literatures works and try to summarized its and compare stages in two systems. Moreover, Table 2 showed performance of these techniques based on handcraft feature extraction methods which is utilized in previous literatures works and try to summarized its.

Table 1. Summarized CAD systems depends on feature extraction methods

Stages	CAD system utilized handcraft or traditional feature extraction (first module)	CAD system based on automatic feature extraction (utilized deep learning) (the second module)	Note
Noise denoising and image enhancements Filters	The log filter, Gaussian and median filter, and Dot Enhancement filter, Wiener filter, multi-scale filter, Gabor filter, Sell filter, LBP, Fuzzy and sequential filter.	Croup, Zooming, Normalization, resizing images.	This stage deals with reducing noise to CT scan images and try to enhance images by applied different filters. This step as we noticed used in the first (handcraft) model widely, because the best results, can be obtained in the next segmentation steps if the quality of the images is increased. However, second model system scan images as pixel by pixel and take a decision so it is not preferred to use these filters but utilized some preprocessing technique can help in the auto feature detection systems.
Lung Segmentation	3D region-growing algorithm with 3D labeling algorithm, iterative threshold and Otsu threshold, global active contour method, adaptive threshold, adaptive 3-D fuzzy threshold, region and 3D region method, active contour method.	U-net, V-net.	These methods were used to extract the lungs in the first module. Furthermore, the second model implements a neural network to extract nodules.
Feature extraction	Shannon and Tsallis Q entropy, Computed Tomography min value, Computed Tomography max value, volume sphericity, spatial distribution density, and maximum diameter feature, angular histogram of surface normal (AHSN), Diversity index feature.	Ann, CNN	The first module depends on extracting vectors of features depending on shape or texture or intensity or mixed between these types to extract nodules. The second module utilizes a neural network to extract nodules and, after that, decide if it is nodule or non-nodule.
Classification step	Space vector machine (SVM), rule-based classification (RBC), GLMR, K-means classifier, KNN classifier.	Ann, CNN	The first module utilizes different classifiers to predict benign or malignant tissue. The second module depends on a neural network to decided nodules or non-nodule

3. RESULTS AND DISCUSSION

The results as shown in Tables 2 and 3 by applying various kinds, whether it is (handcraft or automatic) CAD system. the results are different some of these research calculates the accuracy and sensitivity and tries to reduce false-positive reduction other research show accuracy only in [53], [68]–[70] or sensitivity and false-positive reduction. Moreover, the results may differ if the dataset change so, this can be made the comparison more complex. Some of the researches in Table 3, as mentioned before, utilized systems and tested them on a single or private dataset like in [50], [52], [70]–[72]. Some of this research adopted competition performance metric (CPM). Other utilized free response receiver operating characteristic (FROC) metrics.

Table 2. Performance for the system in literature based on handcraft features extraction

Reference	Data Sets	Results
[9]	LIDC	Acc.: 99.0% Sens.: 97.5% Spc.: 97.5% FPs=6.76
[25]	LIDC	Acc.: 88.4% Sens.: 90.6% spc.: 85% FPs=1.17
[50]	Privet	Sens.: 85% FPs=2
[51]	LIDC	Acc.: 92% Sens.: 100% spc.: 50% FPs=21
[52]	Privet	Sens.:91.95% FPs=17.64
[54]	LIDC-IDRI	Acc.: 99.2% Sens.: 98% Spc.: 97.6%
[55]	LIDC	Sens.: 89.7% FPs=4.14
[56]	LIDC-IDRI	Acc.: 95.33% Sens.: 91.99% Spc.: 96.48%
[60]	LIDC	Sens.: 97.33 % Spc.: 97.11%
[61]	NSRTC-LUNG/LIDC	Acc.: 87.8 % Sens.: 93.75 % Spc.: 87.6%
[62]	JSRT	Sens.: 78.1
[68]	LIDC	Acc.: 91.00
[69]	JSRT	Acc.: 96.58
[71]	University of Istanbul	Acc.: 90.7 % Sens.: 89.6% Spc.: 87.5%
[73]	LIDC-IDRI	Acc.: 97.55 % Sens.: 85.91 % Spc.: 97.7%
[74]	LIDC-IDRI	Acc.: 80.36% Sens.: 82.05 % Spc.: 76.47%
[75]	NBIA/ELCAP	Acc.: 82.66% Sens.: 96.15 % Spc.: 52.17%
[76]	3AHG	Acc.: 84.39 % Spc.: 92%

Table 3. Review for results and networks architecture to CNN in literature

References	Network	Data set	Result
[63]	2D CNN	LIDC	Acc.: 99.51 Sens.: 99.32 Spec.: 99.71
[64]	2D CNN	LIDC dataset	Sens: 85.256% Spec.: 90.658% Acc.: 89.895% AUC: 0.94
[65]		Luna	Acc.: 91.23 Sens.: 81.2
[66]	M-RPN 3D DCNN	Sph6 &LIDC-IDRI& ANODE09 &LUNA 16	Sens.: 98.4% and 98.7% at 2.1 and FPs/scan: 1.97 FROC score 0.946
[67]	MBEL-3D CNN	LUNA 16	CPM score 87.3%
[70]	2D CNN	Italian MLD & Danish DLCST	Acc.: 72.9%
[72]	3D CNN	Privet	Sens.: 90% FPS/scan: 5
[77]	3D Faster R-CNN	LIDC	CPM score 0.550
[78]	3D Faster R-CNN & CMixNet	LIDC-IDRI &LUNA 16	FROC score 94.21%
[79]	PSO CNN	LIDC-IDRI	Acc.: 97.62 Sens.: 92.20 Spec.: 98.21
[80]	3D Faster R-CNN	LIDC-IDRI &LUNA 16	FROC score 84.42%
[81]	2D-CNN	LIDC-IDRI	Acc.: 88.28% Sens.: 83.82% F score 83.45% AUC 87%
[82]	Ensemble of 3D-CNNs	LIDC-IDRI	Acc.: 97.35% Sens.: 96.57% F score 96.42 % AUC 0.98
[83]	CNN	LIDC-IDRI	Acc.: 84.15% Sens.: 83.96% Spec.: 84.32%
[84]	2D- CNN	LIDC	Acc.: 93.20% Sens.: 92.40% Spec.: 94.80% Fps 4.5
[85]	CNN	LIDC-IDRI	Sens.: 80.06% at 4.7 FPs/scan and 94% at 15.1 FPs/scan
[86]	3D CNN	LIDC dataset.	Sens.: 80% FPs/scan: 22.4
[87]	3D CNN	LIDC dataset	For 3D MVCNN with DAG architecture: Sens.: 95.68% Spec.: 94.51% Error rate: 4.59
[88]	3D CNN	LIDC dataset	Acc.: 87.14% Sens: 0.77 Spec: 0.93 AUC: 0.93
[89]	MVCNN	DLCST&ANODE09	Sens.: 85.4% at 1 FPs/scan and 90% at 4 FPs/scan CMP score 0.637
[90]		LIDC	Sens.:92.2
[91]		Private	Sens.:90.1
[92]		LIDC-IDRI	Acc.: 84 Sens.:89
[93]		Luna	Sens.:90.7%
[94]	3D CNN	SPIE-LUNGSx dataset	Sens.: 80% FPs/scan: 10
[95]	2D CNN	LIDC dataset	Acc.: 70.69 % AUC: 0.63
[96]	2D- CNN	LIDC	Acc.: 97.52% Sens.:95.31% Spec.:99.73%
[97]	3D-CNN	LIDC	Acc.: 87.50% Sens.:98.30% Spec.:77.60% FPs/scan: 11

4. CONCLUSION

Firstly, the handcraft or traditional feature extraction are concluded as shown in this paper. The denoising step and enhancement image are important and can assume to reduce false-positive reduction in these CAD systems' next steps. The two lungs are extracted in lung segmentation steps, and some noise and air from the CT scan are removed. The extracted lungs feed to the next step to extract features which in turn contributes to nodule detection later. Moreover, Feature extraction steps are utilized to extract vectors of feature to extract nodules from segmented lungs. This step reduces the false-positive nodules through utilizing different kinds of the feature, as mentioned before in this paper. Finally, the classification step utilizes different classifiers to detect nodules and reduce the false-positive nodules and satisfied if tissue is benign or malignant. Secondly, this paper discussed types of automatic feature extraction systems which utilize deep learning analysis. This system takes image pixels by to analyze them. More computation is required especially when CNN is adopted to extract nodules. This type of system may not require complex denoising and image enhancing methods, but rather some image preprocessing techniques such as zooming, cropping, or rotating images in different directions, which improves diagnosis efficiency. The automatic feature extraction system adopts U-net to segment lungs and nodules masks from its. After that, feed the extracted nodules by U-net to another neural network to make diagnoses if this tissue is benign or malignant. On the other hand, in some literature, CNN 2D and 3D are utilized directly after preprocessing step. In conclusion, Different systems have been developed in lung nodule detection and diagnosis in the last few years, and much research tries to contribute to enhancing the detection and diagnosis of lung nodules systems. Although research tries to detect normal nodules with a size range from 3 to 30 mm, on the other hand, much research focused on nodules with a small radius. Despite these varieties of systems and much research, this topic still needs to be developed in techniques spatially in lung segmentation and reduce false positive detection. This paper's contribution summarized two CAD systems classified on how features have been extracted since 2008 and exhibited some detail about each step for these systems. Finally, the urgent and renewed need for a system used with more than one database with promising results in terms of accuracy, sensitivity, and the rest of the outcome factors.

REFERENCES

- [1] S. L. Armato III *et al.*, "Data from LIDC-IDRI," *The Cancer Imaging Archive (TCIA) Public Access*, 2015, doi: 10.7937/K9/TCIA.2015.LO9QL9SX.
- [2] B. van Ginneken *et al.*, "Comparing and combining algorithms for computer-aided detection of pulmonary nodules in computed tomography scans: The ANODE09 study," *Medical Image Analysis*, vol. 14, no. 6, pp. 707–722, 2010, doi: 10.1016/j.media.2010.05.005.
- [3] M. Kubo *et al.*, "CAD system for lung cancer based on low-dose single-slice CT image," in *Medical Imaging 2002: Image Processing*, 2002, vol. 4684, p. 1262, doi: 10.1117/12.467086.
- [4] R. Nagata, T. Kawaguchi, and H. Miyake, "Automated detection of lung nodules in chest radiographs using a false-positive reduction scheme based on template matching," in *2012 5th International Conference on Biomedical Engineering and Informatics, BMEI 2012*, 2012, pp. 216–223, doi: 10.1109/BMEI.2012.6512916.
- [5] Q. Shi, W. Desheng, C. Ying, and F. Jun, "Lung nodules detection in CT images using gestalt-based algorithm," *Chinese Journal of Electronics*, vol. 25, no. 4, pp. 711–718, 2016, doi: 10.1049/cje.2016.07.009.
- [6] P. B. Sangamithraa and S. Govindaraju, "Lung tumour detection and classification using EK-Mean clustering," in *Proceedings of the 2016 IEEE International Conference on Wireless Communications, Signal Processing and Networking, WiSPNET 2016*, 2016, pp. 2201–2206, doi: 10.1109/WiSPNET.2016.7566533.
- [7] T. Aggarwal, A. Furqan, and K. Kalra, "Feature extraction and LDA based classification of lung nodules in chest CT scan images," in *2015 International Conference on Advances in Computing, Communications and Informatics, ICACCI 2015*, 2015, pp. 1189–1193, doi: 10.1109/ICACCI.2015.7275773.
- [8] S. Soltaninejad, M. Keshani, and F. Tajeripour, "Lung nodule detection by KNN classifier and active contour modelling and 3D visualization," in *AISP 2012 - 16th CSI International Symposium on Artificial Intelligence and Signal Processing*, 2012, pp. 440–445, doi: 10.1109/AISP.2012.6313788.
- [9] W.-J. Choi and T.-S. Choi, "Automated pulmonary nodule detection based on three-dimensional shape-based feature descriptor," *Computer Methods and Programs in Biomedicine*, vol. 113, no. 1, pp. 37–54, Jan. 2014, doi: 10.1016/j.cmpb.2013.08.015.
- [10] S. Sun, W. Gu, L. Fan, and H. Ren, "Detect GGO nodule based on dot filter," in *Proceedings - 2012 International Conference on Biomedical Engineering and Biotechnology, iCBEB 2012*, 2012, pp. 765–767, doi: 10.1109/iCBEB.2012.129.
- [11] H. Shao, L. Cao, and Y. Liu, "A detection approach for solitary pulmonary nodules based on CT images," in *Proceedings of 2nd International Conference on Computer Science and Network Technology, ICCSNT 2012*, 2012, pp. 1253–1257, doi: 10.1109/ICCSNT.2012.6526151.
- [12] S. Takemura, X. Han, Y. W. Chen, K. Ito, I. Nishikwa, and M. Ito, "Enhancement and detection of lung nodules with multiscale filters in CT images," in *Proceedings - 2008 4th International Conference on Intelligent Information Hiding and Multimedia Signal Processing, IHH-MSP 2008*, 2008, pp. 717–720, doi: 10.1109/IHH-MSP.2008.303.
- [13] P. Xiaomin, G. Hongyu, and D. Jianping, "Computerized detection of lung nodules in CT images by use of multiscale filters and geometrical constraint region growing," in *2010 4th International Conference on Bioinformatics and Biomedical Engineering, iCBBE 2010*, 2010, pp. 1–4, doi: 10.1109/ICBBE.2010.5517771.
- [14] K. Punithavathy, M. M. Ramya, and S. Poobal, "Analysis of statistical texture features for automatic lung cancer detection in PET/CT images," in *Proceedings of 2015 International Conference on Robotics, Automation, Control and Embedded Systems, RACE 2015*, 2015, pp. 1–5, doi: 10.1109/RACE.2015.7097244.
- [15] A. K. Dhara, S. Mukhopadhyay, N. Alam, and N. Khandelwal, "Measurement of spiculation index in 3D for solitary pulmonary

- nodules in volumetric lung CT images,” in *Medical Imaging 2013: Computer-Aided Diagnosis*, Feb. 2013, vol. 8670, doi: 10.1117/12.2006970.
- [16] A. K. Dhara and S. Mukhopadhyay, “A hybrid preprocessing method using geometry based diffusion and elective enhancement filtering for pulmonary nodule detection,” in *Medical Imaging 2012: Computer-Aided Diagnosis*, 2012, vol. 8315, doi: 10.1117/12.911644.
- [17] N. Hadavi, M. J. Nordin, and A. Shojaei-pour, “Lung cancer diagnosis using CT-scan images based on cellular learning automata,” in *2014 International Conference on Computer and Information Sciences, ICCOINS 2014 - A Conference of World Engineering, Science and Technology Congress, ESTCON 2014 - Proceedings*, 2014, pp. 1–5, doi: 10.1109/ICCOINS.2014.6868370.
- [18] F. Xu *et al.*, “A 3D multi-scale block LBP filter for lung nodule enhancement based on the CT images,” in *Proceedings - 2016 9th International Congress on Image and Signal Processing, BioMedical Engineering and Informatics, CISP-BMEI 2016*, 2017, pp. 1376–1380, doi: 10.1109/CISP-BMEI.2016.7852931.
- [19] C. Li, S. Nie, Y. Wang, and X. Sun, “Experimental investigation of fuzzy enhancement for nonsolid pulmonary nodules,” in *Proceedings 2012 IEEE Symposium on Robotics and Applications, ISRA 2012*, 2012, pp. 756–759, doi: 10.1109/ISRA.2012.6219301.
- [20] D. Wang, J. Wang, Y. Du, and P. Tang, “Adaptive solitary pulmonary nodule segmentation for digital radiography images based on random walks and sequential filter,” *IEEE Access*, vol. 5, pp. 1460–1468, 2017, doi: 10.1109/ACCESS.2017.2668523.
- [21] S. van de Leemput, F. Dorsers, and B. Ehteshami Bejnordi, “A novel spherical shell filter for reducing false positives in automatic detection of pulmonary nodules in thoracic CT scans,” in *Medical Imaging 2015: Computer-Aided Diagnosis*, Mar. 2015, vol. 9414, doi: 10.1117/12.2082298.
- [22] J. R. F. da Silva Sousa, A. C. Silva, A. C. de Paiva, and R. A. Nunes, “Methodology for automatic detection of lung nodules in computerized tomography images,” *Computer Methods and Programs in Biomedicine*, vol. 98, no. 1, pp. 1–14, Apr. 2010, doi: 10.1016/j.cmpb.2009.07.006.
- [23] M. P. Paing and S. Choomchuay, “Ground glass opacity (GGO) nodules detection from lung CT scans,” in *2017 International Symposium on Electronics and Smart Devices (ISESD)*, Oct. 2017, pp. 230–235, doi: 10.1109/ISESD.2017.8253338.
- [24] W. Zhang, X. Wang, X. Li, and J. Chen, “3D skeletonization feature based computer-aided detection system for pulmonary nodules in CT datasets,” *Computers in Biology and Medicine*, vol. 92, pp. 64–72, 2018, doi: 10.1016/j.compbiomed.2017.11.008.
- [25] A. M. Santos, A. O. De Carvalho Filho, A. C. Silva, A. C. De Paiva, R. A. Nunes, and M. Gattass, “Automatic detection of small lung nodules in 3D CT data using Gaussian mixture models, Tsallis entropy and SVM,” *Engineering Applications of Artificial Intelligence*, vol. 36, pp. 27–39, 2014, doi: 10.1016/j.engappai.2014.07.007.
- [26] J. J. Suárez-Cuenca *et al.*, “Application of the iris filter for automatic detection of pulmonary nodules on computed tomography images,” *Computers in Biology and Medicine*, vol. 39, no. 10, pp. 921–933, 2009, doi: 10.1016/j.compbiomed.2009.07.005.
- [27] J. Pu, D. S. Paik, X. Meng, J. Roos, and G. D. Rubin, “Shape ‘break-and-repair’ strategy and its application to automated medical image segmentation,” *IEEE Transactions on Visualization and Computer Graphics*, vol. 17, no. 1, pp. 115–124, 2011, doi: 10.1109/TVCG.2010.56.
- [28] M. P. Paing and S. Choomchuay, “Classification of margin characteristics from 3D pulmonary nodules,” in *BMEiCON 2017 - 10th Biomedical Engineering International Conference*, 2017, vol. 2017-Janua, pp. 1–5, doi: 10.1109/BMEiCON.2017.8229104.
- [29] L. Fu, J. Ma, Y. Ren, Y. S. Han, and J. Zhao, “Automatic detection of lung nodules: false positive reduction using convolution neural networks and handcrafted features,” in *Medical Imaging 2017: Computer-Aided Diagnosis*, 2017, vol. 10134, 101340A, doi: 10.1117/12.2253995.
- [30] M. Javid, M. Javid, M. Z. U. Rehman, and S. I. A. Shah, “A novel approach to CAD system for the detection of lung nodules in CT images,” *Computer Methods and Programs in Biomedicine*, vol. 135, pp. 125–139, 2016, doi: 10.1016/j.cmpb.2016.07.031.
- [31] E. Rendon-Gonzalez and V. Ponomaryov, “Automatic lung nodule segmentation and classification in CT images based on SVM,” in *9th International Kharkiv Symposium on Physics and Engineering of Microwaves, Millimeter and Submillimeter Waves, MSMW 2016*, 2016, pp. 1–4, doi: 10.1109/MSMW.2016.7537995.
- [32] S. Saïen, A. Hamid Pilevar, and H. Abrishami Moghaddam, “Refinement of lung nodule candidates based on local geometric shape analysis and laplacian of gaussian kernels,” *Computers in Biology and Medicine*, vol. 54, pp. 188–198, 2014, doi: 10.1016/j.compbiomed.2014.09.010.
- [33] T. Messay, R. C. Hardie, and S. K. Rogers, “A new computationally efficient CAD system for pulmonary nodule detection in CT imagery,” *Medical Image Analysis*, vol. 14, no. 3, pp. 390–406, 2010, doi: 10.1016/j.media.2010.02.004.
- [34] K. Gopi and J. Selvakumar, “Lung tumor area recognition and classification using EK-mean clustering and SVM,” in *2017 International Conference On Nextgen Electronic Technologies: Silicon to Software, ICNETS2 2017*, 2017, pp. 97–100, doi: 10.1109/ICNETS2.2017.8067906.
- [35] W.-J. Choi and T.-S. Choi, “False positive reduction for pulmonary nodule detection using two-dimensional principal component analysis,” in *Applications of Digital Image Processing XXXII*, 2009, vol. 7443, 744322, doi: 10.1117/12.827252.
- [36] W. J. Choi and T. S. Choi, “Genetic programming-based feature transform and classification for the automatic detection of pulmonary nodules on computed tomography images,” *Information Sciences*, vol. 212, pp. 57–78, 2012, doi: 10.1016/j.ins.2012.05.008.
- [37] R. Nurfauzi, H. A. Nugroho, and I. Ardiyanto, “Lung detection using adaptive border correction,” in *Proceeding - 2017 3rd International Conference on Science and Technology-Computer, ICST 2017*, 2017, pp. 57–60, doi: 10.1109/ICSTC.2017.8011852.
- [38] P. Kamra, R. Vishraj, Kanika, and S. Gupta, “Performance comparison of image segmentation techniques for lung nodule detection in CT images,” in *Proceedings of 2015 International Conference on Signal Processing, Computing and Control, ISPCC 2015*, 2016, pp. 302–306, doi: 10.1109/ISPCC.2015.7375045.
- [39] Y. Wei, G. Shen, and J. J. Li, “A fully automatic method for lung parenchyma segmentation and repairing,” *Journal of Digital Imaging*, vol. 26, no. 3, pp. 483–495, 2013, doi: 10.1007/s10278-012-9528-9.
- [40] X. Y. Li, F. Xu, X. Hu, S. H. Peng, H. Do Nam, and J. M. Zhao, “Self-adapting threshold of pulmonary parenchyma,” in *Proceedings - 2016 9th International Congress on Image and Signal Processing, BioMedical Engineering and Informatics, CISP-BMEI 2016*, 2017, pp. 1429–1434, doi: 10.1109/CISP-BMEI.2016.7852941.
- [41] X. Ye, X. Lin, J. Dehmshki, G. Slabaugh, and G. Beddoe, “Shape-based computer-aided detection of lung nodules in thoracic CT images,” *IEEE Transactions on Biomedical Engineering*, vol. 56, no. 7, pp. 1810–1820, 2009, doi: 10.1109/TBME.2009.2017027.
- [42] D. Cascio, R. Magro, F. Fauci, M. Iacomi, and G. Raso, “Automatic detection of lung nodules in CT datasets based on stable 3D mass-spring models,” *Computers in Biology and Medicine*, vol. 42, no. 11, pp. 1098–1109, 2012, doi: 10.1016/j.compbiomed.2012.09.002.

- [43] S. A. El-Regaily, M. A. M. Salem, M. H. A. Aziz, and M. I. Roushdy, "Lung nodule segmentation and detection in computed tomography," in *2017 IEEE 8th International Conference on Intelligent Computing and Information Systems, ICICIS 2017*, 2017, pp. 72–78, doi: 10.1109/INTELCIS.2017.8260029.
- [44] J. Gong, J. yu Liu, L. jia Wang, B. Zheng, and S. dong Nie, "Computer-aided detection of pulmonary nodules using dynamic self-adaptive template matching and a FLDA classifier," *Physica Medica*, vol. 32, no. 12, pp. 1502–1509, 2016, doi: 10.1016/j.ejmp.2016.11.001.
- [45] R. Agarwal, A. Shankhadhar, and R. K. Sagar, "Detection of lung cancer using content based medical image retrieval," in *International Conference on Advanced Computing and Communication Technologies, ACCT*, 2015, vol. 2015-April, pp. 48–52, doi: 10.1109/ACCT.2015.33.
- [46] F. V. Farahani, A. Ahmadi, and M. H. F. Zarandi, "Lung nodule diagnosis from CT images based on ensemble learning," in *2015 IEEE Conference on Computational Intelligence in Bioinformatics and Computational Biology, CIBCB 2015*, 2015, pp. 1–7, doi: 10.1109/CIBCB.2015.7300281.
- [47] S. Sun, W. Li, and Y. Kang, "Lung nodule detection based on GA and SVM," in *Proceedings - 2015 8th International Conference on BioMedical Engineering and Informatics, BMEI 2015*, 2016, pp. 96–100, doi: 10.1109/BMEI.2015.7401480.
- [48] P. Cerello, "The MAGIC-5 CAD for nodule detection in low dose and thin slice lung CTs," *Nuclear Instruments and Methods in Physics Research, Section A: Accelerators, Spectrometers, Detectors and Associated Equipment*, vol. 623, no. 2, pp. 832–835, 2010, doi: 10.1016/j.nima.2010.04.118.
- [49] Q. Abbas, "Segmentation of differential structures on computed tomography images for diagnosis lung-related diseases," *Biomedical Signal Processing and Control*, vol. 33, pp. 325–334, Mar. 2017, doi: 10.1016/j.bspc.2016.12.019.
- [50] J. Tong, W. Ying, and W. C. Dong, "A lung cancer lesions detection scheme based on CT image," in *2010 2nd International Conference on Signal Processing Systems*, 2010, vol. 1, pp. V1-557-V1-560, doi: 10.1109/ICSPS.2010.5555557.
- [51] S. Makaju, P. W. C. Prasad, A. Alsadoon, A. K. Singh, and A. Elchouemi, "Lung cancer detection using CT scan images," *Procedia Computer Science*, vol. 125, pp. 107–114, 2018, doi: 10.1016/j.procs.2017.12.016.
- [52] G. Cao, Y. Liu, and K. Suzuki, "A new method for false-positive reduction in detection of lung nodules in CT images," in *International Conference on Digital Signal Processing, DSP*, 2014, pp. 474–479, doi: 10.1109/ICDSP.2014.6900710.
- [53] E. Taşı and A. Uğur, "Shape and texture based novel features for automated juxtapleural nodule detection in lung CTs," *Journal of Medical Systems*, vol. 39, no. 5, May 2015, doi: 10.1007/s10916-015-0231-5.
- [54] A. O. de Carvalho Filho, A. C. Silva, A. C. de Paiva, R. A. Nunes, and M. Gattass, "Lung-nodule classification based on computed tomography using taxonomic diversity indexes and an SVM," *Journal of Signal Processing Systems*, vol. 87, no. 2, pp. 179–196, 2017, doi: 10.1007/s11265-016-1134-5.
- [55] H. Han, L. Li, F. Han, B. Song, W. Moore, and Z. Liang, "Fast and adaptive detection of pulmonary nodules in thoracic CT images using a hierarchical vector quantization scheme," *IEEE Journal of Biomedical and Health Informatics*, vol. 19, no. 2, pp. 648–659, 2015, doi: 10.1109/JBHI.2014.2328870.
- [56] A. O. de C. Filho, A. C. Silva, A. C. de Paiva, R. A. Nunes, and M. Gattass, "3D shape analysis to reduce false positives for lung nodule detection systems," *Medical and Biological Engineering and Computing*, vol. 55, no. 8, pp. 1199–1213, 2017, doi: 10.1007/s11517-016-1582-x.
- [57] G. Litjens *et al.*, "A survey on deep learning in medical image analysis," *Medical Image Analysis*, vol. 42, pp. 60–88, 2017, doi: <https://doi.org/10.1016/j.media.2017.07.005>.
- [58] K. K. L. Wong, L. Wang, and D. Wang, "Recent developments in machine learning for medical imaging applications," *Computerized Medical Imaging and Graphics*, vol. 57, no. 57, pp. 1–3, Apr. 2017, doi: 10.1016/j.compmedimag.2017.04.001.
- [59] M. de Bruijne, "Machine learning approaches in medical image analysis: From detection to diagnosis," *Medical Image Analysis*, vol. 33, Elsevier, pp. 94–97, 2016, doi: 10.1016/j.media.2016.06.032.
- [60] S. L. A. Lee, A. Z. Kouzani, and E. J. Hu, "Random forest based lung nodule classification aided by clustering," *Computerized Medical Imaging and Graphics*, vol. 34, no. 7, pp. 535–542, 2010, doi: 10.1016/j.compmedimag.2010.03.006.
- [61] Y. Liu, J. Yang, D. Zhao, and J. Liu, "Computer aided detection of lung nodules based on voxel analysis utilizing support vector machines," in *FBIE 2009 - 2009 International Conference on Future BioMedical Information Engineering*, 2009, pp. 90–93, doi: 10.1109/FBIE.2009.5405784.
- [62] R. C. Hardie, S. K. Rogers, T. Wilson, and A. Rogers, "Performance analysis of a new computer aided detection system for identifying lung nodules on chest radiographs," *Medical Image Analysis*, vol. 12, no. 3, pp. 240–258, 2008, doi: 10.1016/j.media.2007.10.004.
- [63] M. Toğaçar, B. Ergen, and Z. Cömert, "Detection of lung cancer on chest CT images using minimum redundancy maximum relevance feature selection method with convolutional neural networks," *Biocybernetics and Biomedical Engineering*, vol. 40, no. 1, pp. 23–39, 2020, doi: 10.1016/j.bbe.2019.11.004.
- [64] S. A. El-Regaily, M. A. M. Salem, M. H. Abdel Aziz, and M. I. Roushdy, "Multi-view convolutional neural network for lung nodule false positive reduction," *Expert Systems with Applications*, vol. 162, p. 113017, 2020, doi: 10.1016/j.eswa.2019.113017.
- [65] P. Moradi and M. Jamzad, "Detecting lung cancer lesions in CT images using 3D convolutional neural networks," in *4th International Conference on Pattern Recognition and Image Analysis, IPRIA 2019*, 2019, pp. 114–118, doi: 10.1109/PRIA.2019.8785971.
- [66] A. Masood *et al.*, "Cloud-based automated clinical decision support system for detection and diagnosis of lung cancer in chest CT," *IEEE Journal of Translational Engineering in Health and Medicine*, vol. 8, pp. 1–13, 2020, doi: 10.1109/JTEHM.2019.2955458.
- [67] H. Cao *et al.*, "Multi-branch ensemble learning architecture based on 3D CNN for false positive reduction in lung nodule detection," *IEEE Access*, vol. 7, pp. 67380–67391, 2019, doi: 10.1109/ACCESS.2019.2906116.
- [68] C. F. J. Kuo *et al.*, "Automatic lung nodule detection system using image processing techniques in computed tomography," *Biomedical Signal Processing and Control*, vol. 56, p. 101659, 2020, doi: 10.1016/j.bspc.2019.101659.
- [69] H. R. H. Al-Absi, B. B. Samir, K. B. Shaban, and S. Sulaiman, "Computer aided diagnosis system based on machine learning techniques for lung cancer," in *2012 International Conference on Computer and Information Science, ICCIS 2012 - A Conference of World Engineering, Science and Technology Congress, ESTCON 2012 - Conference Proceedings*, 2012, vol. 1, pp. 295–300, doi: 10.1109/ICCISci.2012.6297257.
- [70] F. Ciompi *et al.*, "Corrigendum: Towards automatic pulmonary nodule management in lung cancer screening with deep learning," *Scientific reports*, vol. 7, p. 46878, 2017, doi: 10.1038/srep46878.
- [71] A. Tartar, N. Kilic, and A. Akan, "Classification of pulmonary nodules by using hybrid features," *Computational and Mathematical Methods in Medicine*, vol. 2013, 2013, doi: 10.1155/2013/148363.
- [72] X. Huang, J. Shan, and V. Vaidya, "Lung nodule detection in CT using 3D convolutional neural networks," in *Proceedings - International Symposium on Biomedical Imaging*, 2017, pp. 379–383, doi: 10.1109/ISBI.2017.7950542.

- [73] A. O. De Carvalho Filho, W. B. De Sampaio, A. C. Silva, A. C. de Paiva, R. A. Nunes, and M. Gattass, "Automatic detection of solitary lung nodules using quality threshold clustering, genetic algorithm and diversity index," *Artificial Intelligence in Medicine*, vol. 60, no. 3, pp. 165–177, 2014, doi: 10.1016/j.artmed.2013.11.002.
- [74] S. Sivakumar and C. Chandrasekar, "Lung nodule detection using fuzzy clustering and support vector machines," *International Journal of Engineering and Technology*, vol. 5, no. 1, pp. 179–185, 2013.
- [75] H. M. Orozco, O. O. V. Villegas, L. O. Maynez, V. G. C. Sanchez, and H. D. J. O. Dominguez, "Lung nodule classification in frequency domain using support vector machines," in *2012 11th International Conference on Information Science, Signal Processing and their Applications, ISSPA 2012*, 2012, pp. 870–875, doi: 10.1109/ISSPA.2012.6310676.
- [76] J. Zhang, B. Li, and L. Tian, "Lung nodule classification combining rule-based and SVM," in *Proceedings 2010 IEEE 5th International Conference on Bio-Inspired Computing: Theories and Applications, BIC-TA 2010*, 2010, pp. 1033–1036, doi: 10.1109/BICTA.2010.5645114.
- [77] C. Han *et al.*, "Synthesizing diverse lung nodules wherever massively: 3D multi-conditional GAN-based CT image augmentation for object detection," in *Proceedings - 2019 International Conference on 3D Vision, 3DV 2019*, 2019, pp. 729–737, doi: 10.1109/3DV.2019.00085.
- [78] N. Nasrullah, J. Sang, M. S. Alam, M. Mateen, B. Cai, and H. Hu, "Automated lung nodule detection and classification using deep learning combined with multiple strategies," *Sensors*, vol. 19, no. 17, Aug. 2019, doi: 10.3390/s19173722.
- [79] G. L. F. da Silva, T. L. A. Valente, A. C. Silva, A. C. de Paiva, and M. Gattass, "Convolutional neural network-based PSO for lung nodule false positive reduction on CT images," *Computer Methods and Programs in Biomedicine*, vol. 162, pp. 109–118, 2018, doi: 10.1016/j.cmpb.2018.05.006.
- [80] W. Zhu, C. Liu, W. Fan, and X. Xie, "DeepLung: Deep 3D dual path nets for automated pulmonary nodule detection and classification," in *Proceedings - 2018 IEEE Winter Conference on Applications of Computer Vision, WACV 2018*, 2018, vol. 2018-Janua, pp. 673–681, doi: 10.1109/WACV.2018.00079.
- [81] S. Sun, W. Li, and Y. Kang, "Lung nodule detection based on GA and SVM," in *2015 8th International Conference on Biomedical Engineering and Informatics (BMEI)*, Oct. 2015, vol. 17, no. 1, pp. 96–100, doi: 10.1109/BMEI.2015.7401480.
- [82] P. Monkam *et al.*, "Ensemble learning of multiple-view 3D-CNNs model for micro-nodules identification in CT images," *IEEE Access*, vol. 7, pp. 5564–5576, 2019, doi: 10.1109/ACCESS.2018.2889350.
- [83] Q. Song, L. Zhao, X. Luo, and X. Dou, "Using deep learning for classification of lung nodules on computed tomography images," *Journal of Healthcare Engineering*, vol. 2017, pp. 1–7, 2017, doi: 10.1155/2017/8314740.
- [84] J. kui Liu *et al.*, "An assisted diagnosis system for detection of early pulmonary nodule in computed tomography images," *Journal of Medical Systems*, vol. 41, no. 2, p. 30, 2017, doi: 10.1007/s10916-016-0669-0.
- [85] H. Jiang, H. Ma, W. Qian, M. Gao, and Y. Li, "An Automatic detection system of lung nodule based on multigroup patch-based deep learning network," *IEEE Journal of Biomedical and Health Informatics*, vol. 22, no. 4, pp. 1227–1237, Jul. 2018, doi: 10.1109/JBHI.2017.2725903.
- [86] S. Hamidian, B. Sahiner, N. Petrick, and A. Pezeshk, "3D convolutional neural network for automatic detection of lung nodules in chest CT," in *Medical Imaging 2017: Computer-Aided Diagnosis*, 2017, vol. 10134, 1013409.
- [87] K. Liu and G. Kang, "Multiview convolutional neural networks for lung nodule classification," *International Journal of Imaging Systems and Technology*, vol. 27, no. 1, pp. 12–22, 2017, doi: 10.1002/ima.22206.
- [88] W. Shen *et al.*, "Multi-crop convolutional neural networks for lung nodule malignancy suspiciousness classification," *Pattern Recognition*, vol. 61, pp. 663–673, 2017, doi: <https://doi.org/10.1016/j.patcog.2016.05.029>.
- [89] A. A. A. Setio *et al.*, "Pulmonary nodule detection in CT images: False positive reduction using multi-view convolutional networks," *IEEE Transactions on Medical Imaging*, vol. 35, no. 5, pp. 1160–1169, 2016, doi: 10.1109/TMI.2016.2536809.
- [90] Q. Dou, H. Chen, L. Yu, J. Qin, and P. A. Heng, "Multilevel contextual 3-D CNNs for false positive reduction in pulmonary nodule detection," *IEEE Transactions on Biomedical Engineering*, vol. 64, no. 7, pp. 1558–1567, 2017, doi: 10.1109/TBME.2016.2613502.
- [91] A. Teramoto, H. Fujita, O. Yamamuro, and T. Tamaki, "Automated detection of pulmonary nodules in PET/CT images: Ensemble false-positive reduction using a convolutional neural network technique," *Medical Physics*, vol. 43, no. 6, pp. 2821–2827, 2016, doi: 10.1118/1.4948498.
- [92] W. Li, P. Cao, D. Zhao, and J. Wang, "Pulmonary nodule classification with deep convolutional neural networks on computed tomography images," *Computational and Mathematical Methods in Medicine*, vol. 2016, pp. 1–7, 2016, doi: 10.1155/2016/6215085.
- [93] M. Sakamoto and H. Nakano, "Cascaded neural networks with selective classifiers and its evaluation using lung X-ray CT images," *arXiv preprint arXiv:1611.07136*, 2016.
- [94] R. Anirudh, J. J. Thiagarajan, T. Bremer, and H. Kim, "Lung nodule detection using 3D convolutional neural networks trained on weakly labeled data," in *Medical Imaging 2016: Computer-Aided Diagnosis*, 2016, vol. 9785, 978532, doi: 10.1117/12.2214876.
- [95] W. Shen *et al.*, "Learning from experts: developing transferable deep features for patient-level lung cancer prediction," in *Lecture Notes in Computer Science (including subseries Lecture Notes in Artificial Intelligence and Lecture Notes in Bioinformatics)*, Springer, 2016, pp. 124–131.
- [96] A. Sheeraz, J. M. Younus, A. M. Usman, Q. Usman, and H. Ali, "Pulmonary nodules detection and classification using hybrid features from computerized tomographic images," *Journal of Medical Imaging and Health Informatics*, vol. 6, no. 1, pp. 252–259, 2016, doi: 10.1166/jmihi.2016.1600.
- [97] N. Manikandan and K. Devi, "Automatic detection and classification of pulmonary nodules on CT images," *Research Journal of Engineering and Technology*, vol. 5, no. 2, pp. 68–76, 2014.

BIOGRAPHIES OF AUTHORS

Omar Raad Kadhim     received B.Sc. in electronic and communication engineering from University of Baghdad, Baghdad, Iraq in 2009 and M.Sc. in Electronic and Communication Engineering from Cankaya University, Ankara, and turkey in 2014. And now he is a Ph.D. student in electrical engineering department in Babylon University, Babylon, Iraq. At the same time, he is assistant lecturer in Al-Iraqia University, Baghdad, Iraq. His research interests include image processing, channel coding, RF communication, electronics, analog and digital signal processing, and analog integrated circuit design. He can be contacted at email: omaryo.omar@gmail.com.



Hassan Jassim Motlak     received B.Sc. in electrical engineering and M.Sc. in Electrical Engineering from University of Babylon, Babylon, Iraq and Ph.D. from Jamia Millia Islamia, Delhi, India. He has been with Department of Electrical Engineering, Engineering College, University of Babylon, Iraq. His scientific degree is Professor and research interests include communication electronics, analog and digital signal processing, and analog integrated circuit design. He can be contacted at email: hssn_jasim@yahoo.com.



Kasim Karam Abdalla     received B.Sc. in electrical engineering and M.Sc. in Communication Engineering from University of Technology, Baghdad, Iraq and Ph.D. from Jamia Millia Islamia, Delhi, India. He has been with Department of Electrical Engineering, Engineering College, University of Babylon, Iraq since 2006. His scientific degree is Professor and research interests include communication electronics, analog and digital signal processing, and analog integrated circuit design. He can be contacted at email: kasimkaa.11@gmail.com